

Long non-coding RNA OIP5-AS1 promotes cell proliferation and aerobic glycolysis in gastric cancer through sponging miR-186

Jiaobao Huang, Shuangshuang Hou, Jian Xu, Ju Wu, Jiajun Yin

Department of General Surgery, Affiliated Zhongshan Hospital of Dalian University, Dalian, China

Submitted: 3 July 2018; **Accepted:** 9 November 2018

Online publication: 15 August 2019

Arch Med Sci 2021; 17 (6): 1742–1751

DOI: <https://doi.org/10.5114/aoms.2019.87213>

Copyright © 2019 Termedia & Banach

Corresponding author:

Jiajun Yin
Department
of General Surgery
Affiliated Zhongshan Hospital
of Dalian University
6 Jiefang Road
Zhongshan, Dalian
Liaoning, China
Phone: 0411-62893000
E-mail: poyejo7@163.com

Abstract

Introduction: Long non-coding RNAs (lncRNAs) play vital roles in tumour initiation and progression. lncRNA OIP5-AS1 is a potential oncogene in many types of human malignancies, but its biological functions in gastric cancer (GC) remain to be further elucidated.

Material and methods: The expression levels of OIP5-AS1 and miR-186 in GC tissues and cell lines were detected by RT-qPCR analysis. CCK-8 assay and colony formation assay were performed to investigate the proliferation of GC cells *in vitro*, and a nude mouse tumour model was established to validate the role of OIP5-AS1 in GC tumorigenesis *in vivo*. The glucose consumption and lactate production of GC cells were detected by ELISA assay. Interaction between OIP5-AS1 and miR-186 was determined using dual luciferase reporter assay.

Results: The results demonstrated that OIP5-AS1 was upregulated in GC tissues and cell lines and that its high expression was notably correlated with aggressive clinicopathological features of GC patients. Functionally, knockdown of OIP5-AS1 inhibited GC cell proliferation and enhanced cell apoptosis *in vitro*, and inhibited GC xenograft growth *in vivo*. In addition, knockdown of OIP5-AS1 reduced the glucose consumption and lactate production in GC cells. In particular, OIP5-AS1 may function as a ceRNA for miR-186, and inhibition of miR-186 blocks the effects of OIP5-AS1 knockdown on aerobic glycolysis in GC cells.

Conclusions: Accordingly, our findings suggested that the OIP5-AS1/miR-186 axis might be considered as a potential therapeutic target for GC patients.

Key words: long non-coding RNA, gastric cancer, OIP5-AS1, microRNA-186, aerobic glycolysis.

Introduction

Gastric cancer (GC) remains one of the common causes of cancer-related death around the world, particularly in China [1]. At present, surgical resection is still the main therapeutic option for GC treatment. Despite great achievements made in diagnostic and therapeutic methods for GC over the past several decades, the prognostic outcomes of patients with GC remain unsatisfactory [2]. Therefore, there is an urgent need for both clinical surgeons and basic medical researchers to investigate molecular mechanisms that are involved in GC progression.

As a multistep process, gastric carcinogenesis is caused by the accumulation of numerous genetic and epigenetic aberrations. Long non-cod-

ing RNAs (lncRNAs) are a group of non-coding RNA molecules that are greater than 200 nucleotides in length [3], and a handful of published articles have implied that lncRNAs serve pivotal roles in many human diseases, including tumorigenesis [4]. OIP5-AS1, a newly identified lncRNA that is transcribed from Opa-interacting protein 5 (OIP5) gene in antisense orientation [5], has been identified as an oncogene in many types of human cancers, such as lung cancer [6, 7], glioma [8], and hepatoblastoma [9]. Nonetheless, the understanding about the role of OIP5-AS1 in GC progression is still limited.

Therefore, the purpose of the present research is to determine the expression profile and clinical significance of OIP5-AS1 in GC, and to confirm its biological functions in regulating GC cell phenotypes. We believe our study might contribute to the identification of lncRNA-directed diagnostic and therapeutic methods for GC.

Material and methods

Tissue samples

Paired GC and matched adjacent nontumour tissues were collected from 89 patients who underwent primary surgical resection at the Affiliated Zhongshan Hospital of Dalian University (Dalian, China) 2015–2017. All patients did not

receive chemotherapy or radiotherapy prior to the surgery. The clinicopathological characteristics of these patients are listed in Table I. The tissue samples were snap-frozen in liquid nitrogen and then stored at -80°C for further analysis. The research protocols were approved by the Ethics Committee of the Affiliated Zhongshan Hospital of Dalian University, and every patient was asked to sign a written, informed consent form.

Cell culture and transfection

Five GC cell lines (AGS, HGC-27, BGC-823, MGC-803, and SGC-7901) and normal human gastric mucosa cells GES-1, purchased from the Cell Bank of the Chinese Academy of Sciences (Shanghai, China), were cultured in RPMI 1640 medium (Key-Gene, Nanjing, China) containing 10% foetal bovine serum (FBS; Invitrogen, Carlsbad, CA, USA) in a 37°C humidified atmosphere of 5% CO_2 .

Human miR-186 mimics, miR-186 inhibitor, and mimics/inhibitor control were purchased from GenePharma (Shanghai, China), and their sequences were listed in Table II. Knockdown of OIP5-AS1 in cells was obtained by transfection with shRNAs. Chemically synthesised siRNA sequence targeting OIP5-AS1 and the control sequence were inserted into the shRNA expression vector pGPH1/Neo (GenePharma). The sequences of sh-OIP5-AS1

Table I. Relationship between OIP5-AS1 expression and clinicopathological characteristics of GC patients ($n = 89$)

Characteristics	Total number ($n = 89$)	OIP5-AS1 expression		P-value
		Low ($n = 43$)	High ($n = 46$)	
Age [years]:				0.330
≤ 55	47	25	22	
> 55	42	18	24	
Gender:				0.655
Male	60	28	32	
Female	29	15	14	
Tumour size [cm]:				0.036
< 5	52	30	22	
≥ 5	37	13	24	
Histological type:				0.491
Intestinal	71	33	38	
Diffuse	18	10	8	
TNM stage:				0.007
I–II	49	30	19	
III–IV	40	13	27	
Lymph node metastasis:				0.119
Yes	53	22	31	
No	36	21	15	

Table II. The sequences of oligonucleotides and PCR primers

Name	Sequence
miR-186 mimics	CAAAGAAUUCUCCUUUUGGGCUU
miR-186 inhibitor	GUUUCUUUAGAGGAAAACCCGAA
Mimics/inhibitor control	CAGUACUUUUGUGUAGUACAA
OIP5-AS1 forward primer	TGCGAAGATGGCGGAGTAAG
OIP5-AS1 reverse primer	TAGTTCCTCTCTCTGGCCG
GAPDH forward primer	CTCTGCTCCTCTGTTTCGAC
GAPDH reverse primer	CGACCAAATCCGTTGACTCC
miR-186-RT	GTCGTATCCAGTGCAGGGTCCGAGGTATTCGCACTGGATACGACAGCCCA
miR-186 forward primer	CAAAGAATTCTCCTTT
miR-186 reverse primer	GTGCAGGGTCCGAGGT
U6-RT	GTCGTATCCAGTGCAGGGTCCGAGGTATTCGCACTGGATACGACAAAATA
U6 forward primer	CTCGCTTCGGCAGCACATATACT
U6 reverse primer	ACGCTTCACGAATTTGCGTGTC

were sense: 5'-CACCGCTCCTAGGATCCAGTTATC-CGAAGATAACTGGAATCCTAGGAGC-3'; antisense: 5'-AAAAGCTCCTAGGATCCAGTTATCTTCGGATA-ACTGGAATCCTAGGAGC-3'. Cell transfection was performed using Lipofectamine 3000 (Invitrogen) following the manufacturer's protocol.

RT-qPCR analysis

Total RNA samples were extracted from tissues and cells using TRIzol reagent (Invitrogen). After reverse transcription of the total RNA using a PrimeScript RT reagent Kit (TaKaRa, Dalian, China), qPCR analysis was performed using SYBR Premix Ex Taq (TaKaRa) on an ABI 7500 real-time PCR system (Life Technologies, Carlsbad, CA, USA). GAPDH or U6 was used as an endogenous control. Expression fold changes were calculated by the $2^{-\Delta\Delta Ct}$ method [10]. The formula is as follows:

$$\Delta\Delta Ct = [Ct_{\text{target gene}} - Ct_{\text{GAPDH/U6}}]_{\text{experimental}} - [Ct_{\text{target gene}} - Ct_{\text{GAPDH/U6}}]_{\text{control}}$$

The sequences of PCR primers are listed in Table II.

Western blot analysis

Total proteins were extracted using a protein extraction kit (CW BIO, Beijing, China). Equal amounts of protein were run on SDS-PAGE and then transferred onto PVDF membranes (Millipore, Bedford, MA, USA). The membranes were blocked with 5% milk at room temperature for 1 h, incubated with specific primary antibodies overnight at 4°C, and then incubated with appropriate HRP-conjugated secondary antibodies for 1 h at room temperature. The signals were visualised using an enhanced chemiluminescent detection kit

(Pierce, Rockford, IL, USA), and GAPDH was considered as an internal loading control

Xenograft animal model

Twelve male athymic BALB/c nude mice (4–6 weeks old) were purchased from Vital River Laboratory Animal Technology Co., Ltd. (Beijing, China). AGS cells (5×10^6) stably transfected with sh-OIP5-AS1 or sh-NC were resuspended in 150 μ l of medium and injected subcutaneously into the flank region of the nude mice ($n = 6$ /group). When the tumour volume reached approximately 100 mm³, the tumour growth was monitored every 3 days, and the tumour volume was calculated using the formula: volume = length \times (width)²/2. Three weeks later, mice were sacrificed by carbon dioxide asphyxiation and tumours were dissected. All experimental procedures were approved by the Ethics Committee of Zhongshan Hospital Affiliated of Dalian University, and all efforts were made to minimise animal suffering.

Cell counting kit-8 assay

Cell proliferation was analysed by cell counting kit-8 (CCK-8) assay (Beyotime, Shanghai, China). Following transfection, cells were seeded at a density of 5×10^3 cells/well in 96-well plates and cultured for indicated periods. 10 μ l of CCK-8 solution was added to each well, and the plate was incubated at 37°C for an additional 2 h. The absorbance values were detected at 450 nm using a microplate reader (BioTek Instruments, Inc., Winooski, VT, USA).

Colony formation assay

Approximately 1000 cells were plated into six-well plates and allowed to grow in RPMI-1640 medium containing 10% FBS at 37°C. Culture medium was replaced every 3 days. Twelve days later, the cells were fixed with methanol, stained with 0.1% crystal violet, and observed.

Cell apoptosis analysis

Cell apoptosis was detected using an Annexin V-FITC Apoptosis Detection Kit (Beyotime, Shanghai, China). Briefly, cells were harvested and resuspended in 100 µl binding buffer containing 5 µl of Annexin V-FITC and 5 µl of PI, and then incubated at room temperature in the dark for 15 min. The percentage of apoptotic cells was analysed by flow cytometry (BD Biosciences, Franklin lakes, NJ, USA).

Glucose consumption and lactate production assay

To detect the levels of glucose and lactate, the cellular supernatants were collected after centrifugation and analysed using glucose and lactate assay kits (BioVision, Milpitas, CA, USA) following the manufacturer's protocol. Glucose consumption and lactate production were calculated based on the standard curve.

Dual luciferase reporter assay

The OIP5-AS1 fragment containing the miR-186 binding site was amplified by PCR and cloned into the psiCHECK-2 vector (Promega, Madison, WI, USA). The binding site of OIP5-AS1 and miR-186 was mutated from AUUCUUU to AAUCAAU using a QuickChange® Site-Directed Mutagenesis Kit (Stratagene, La Jolla, CA, USA). Cells were co-transfected with luciferase reporter vectors comprising WT-OIP5-AS1 or MUT-OIP5-AS1 and miR-186 mimics or mimics control using Lipofectamine 3000. The luciferase activities were measured 48 h post-transfection using a dual-luciferase reporter assay system (Promega).

Statistical analysis

Graphpad Prism (version 6.01) software (GraphPad Software, Inc., La Jolla, CA, USA) and SPSS version 18.0 software (SPSS Inc., Chicago, IL, USA) were used for statistical analysis. Experimental data were presented as means ± standard deviation (SD). The differences among the groups were estimated by Student's *t*-test, χ^2 test or one-way ANOVA. Correlation of OIP5-AS1 expression with that of miR-186 was performed by Pearson correlation test. A two-sided *p*-value < 0.05 was considered as statistically significant.

Results

OIP5-AS1 is upregulated in gastric cancer tissues and cell lines

OIP5-AS1 expression was tested in tumour tissues and adjacent nontumor tissues of 89 GC patients by RT-qPCR analysis. Remarkably higher OIP5-AS1 expression was found in GC tissues than that in the adjacent normal tissues (Figure 1 A). We then analysed the association between the OIP5-AS1 expression and clinicopathological features of GC patients. 89 GC patients were allocated into two groups, including a low-expression group (< mean, *n* = 43) and a high-expression group (\geq mean, *n* = 46), according to the cut-off value of OIP5-AS1 expression. Our data showed that high OIP5-AS1 expression was notably correlated with increased tumour size (*p* = 0.036) and advanced TNM stage (*p* = 0.007) (Table I). Then we determined OIP5-AS1 expression in five human GC cell lines. As demonstrated in Figure 1 B, all the GC cell lines showed a notable higher expression level of OIP5-AS1 compared to the normal GES-1 cells.

Knockdown of OIP5-AS1 inhibits gastric cancer cell proliferation and induces cell apoptosis *in vitro*

AGS and SGC-7901 cells showed relatively high expression of OIP5-AS1; therefore, we knocked down the expression of OIP5-AS1 by stable transfection with shRNAs in these cells. As shown in Figure 2 A, OIP5-AS1 expression was significantly reduced after transfection with sh-OIP5-AS1 in AGS and SGC-7901 cells. After OIP5-AS1 knockdown, the proliferation abilities of AGS and SGC-7901 cells were significantly repressed (Figure 2 B). Moreover, the results of colony formation assay indicated that the colony formation rates of AGS and SGC-7901 cells were also markedly suppressed by OIP5-AS1 knockdown (Figure 2 C). Moreover, we also found that OIP5-AS1 knockdown significantly enhanced the apoptosis of AGS and SGC-7901 cells (Figure 2 D).

Knockdown of OIP5-AS1 inhibits GC tumour growth *in vivo*

To further examine the oncogenic role of OIP5-AS1 *in vivo*, a xenograft tumour model was then established. In line with *in vitro* analysis, we found that OIP5-AS1 knockdown remarkably reduced the volume and weight of xenograft tumours (Figures 3 A, B). As confirmed by RT-qPCR analysis, OIP5-AS1 expression was significantly decreased in the tumours formed by sh-OIP5-AS1-transfected cells (Figure 3 C). We also detected the expression levels of apoptosis-associated proteins by western blot analysis, and we found that OIP5-AS1 knockdown

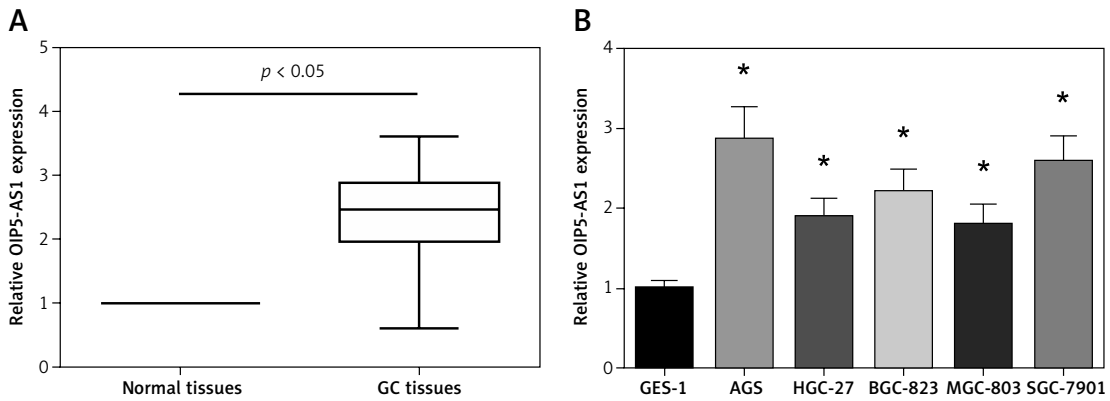


Figure 1. OIP5-AS1 is upregulated in GC tissues and cell lines. **A** – The expression levels of OIP5-AS1 in GC tissues and adjacent nontumour tissues were examined by RT-qPCR analysis. **B** – The expression levels of OIP5-AS1 in five GC cell lines and normal human gastric mucosa cells GES-1 were examined by RT-qPCR analysis

**p* < 0.05 vs. GES-1 cells.

increased Bax expression and decreased Bcl-2 expression in the xenograft tissues (Figure 3 D).

Knockdown of OIP5-AS1 suppresses aerobic glycolysis in gastric cancer cells

Aerobic glycolysis is one of the characteristic phenotypes of cancer cells [11]. As demonstrated in Figures 4 A, B, the glycolytic markers, includ-

ing glucose consumption and lactate production, were all reduced when OIP5-AS1 was knocked down in AGS and SGC-7901 cells.

OIP5-AS1 acts as a ceRNA for miR-186 in gastric cancer cells

Next, we investigated the mechanisms underlying the role of OIP5-AS1. Through starBase v3.0

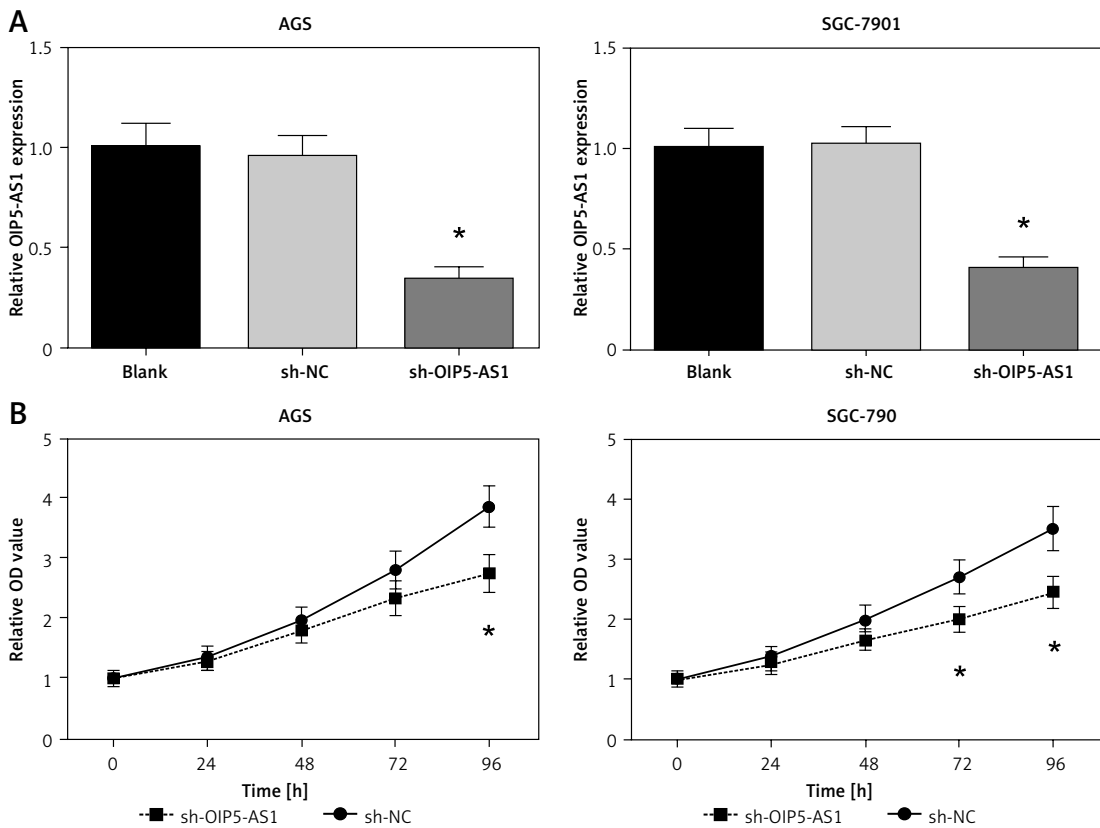


Figure 2. Knockdown of OIP5-AS1 inhibits GC cell proliferation and induces cell apoptosis *in vitro*. **A** – The transfection efficacies in AGS and SGC-7901 cells were determined by RT-qPCR analysis. **B** – The proliferation of AGS and SGC-7901 cells after transfection was determined by CCK-8 assay

**p* < 0.05 vs. sh-NC-transfected cells.

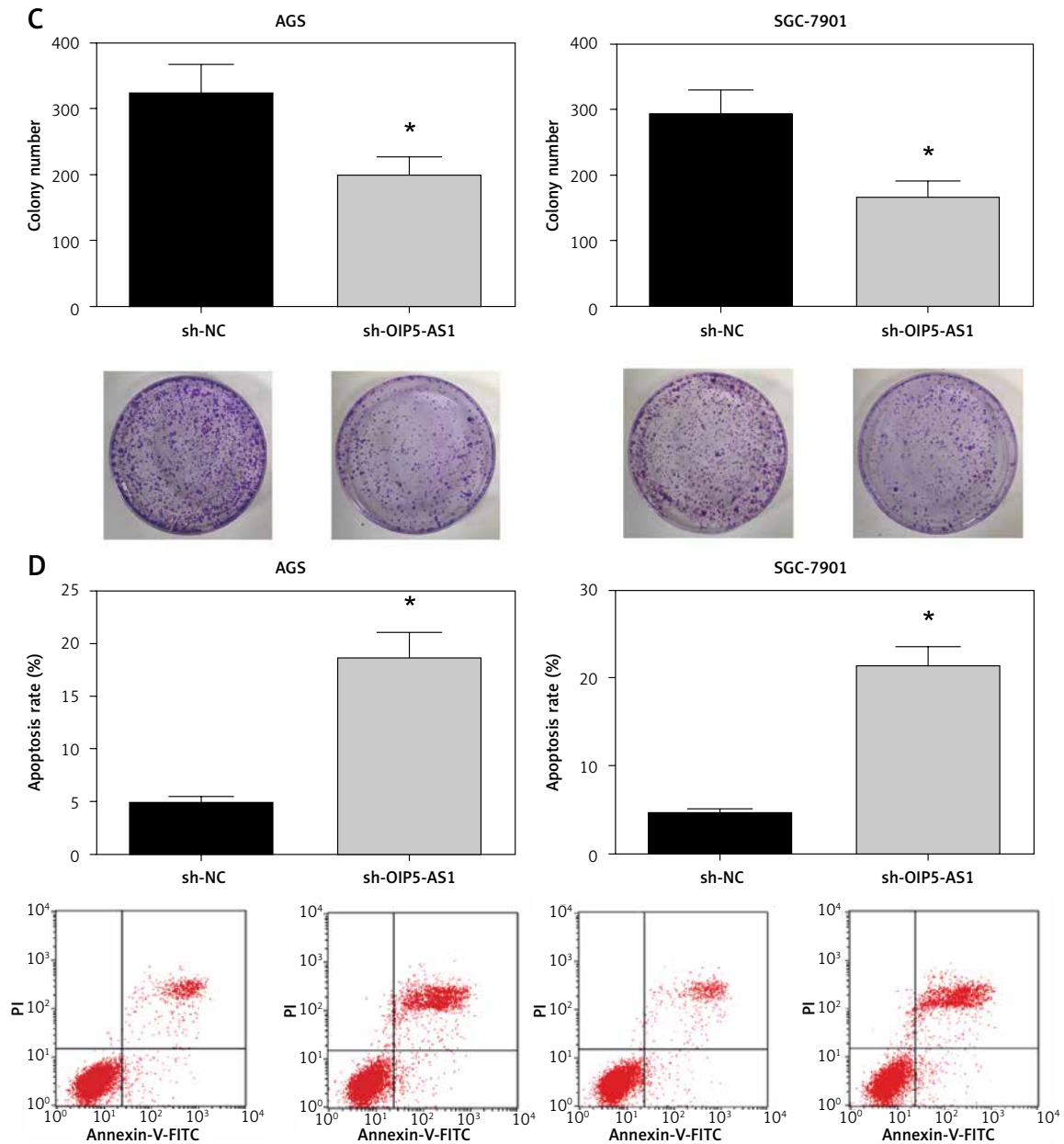


Figure 2. Cont. **C** – The colony formation ability of AGS and SGC-7901 cells after transfection was detected by colony formation assay. **D** – The apoptotic rates of AGS and SGC-7901 cells after transfection were measured by flow cytometry following Annexin-V/PI staining

* $p < 0.05$ vs. sh-NC-transfected cells.

(<http://starbase.sysu.edu.cn/>), we found that miR-186 contains a binding site for OIP5-AS1 (Figure 5A). We further performed dual luciferase reporter assay, and the results indicated that co-transfection with miR-186 mimics markedly inhibited the luciferase activity of OIP5-AS1-WT but not that of OIP5-AS1-MUT in both AGS and SGC-7901 cells (Figure 5B). Also, as shown in Figure 5C, knockdown of OIP5-AS1 remarkably increased miR-186 expression in AGS and SGC-7901 cells. We also observed that miR-186 was downregulated in GC tissues and cell lines (Figures 5D, E). Moreover, as demonstrated in Figure 5F, the expression of

OIP5-AS1 and miR-186 showed a significantly negative correlation in GC tissues ($p = 0.037$).

Inhibition of miR-186 attenuates the effect of OIP5-AS1 knockdown on aerobic glycolysis in gastric cancer cells

We then validated the role of miR-186 in aerobic glycolysis of GC cells. The results demonstrated that co-transfection with miR-186 inhibitor remarkably restored the impaired glucose consumption and lactate production in AGS and SGC-7901 cells with OIP5-AS1 knockdown (Figures 6A, B).

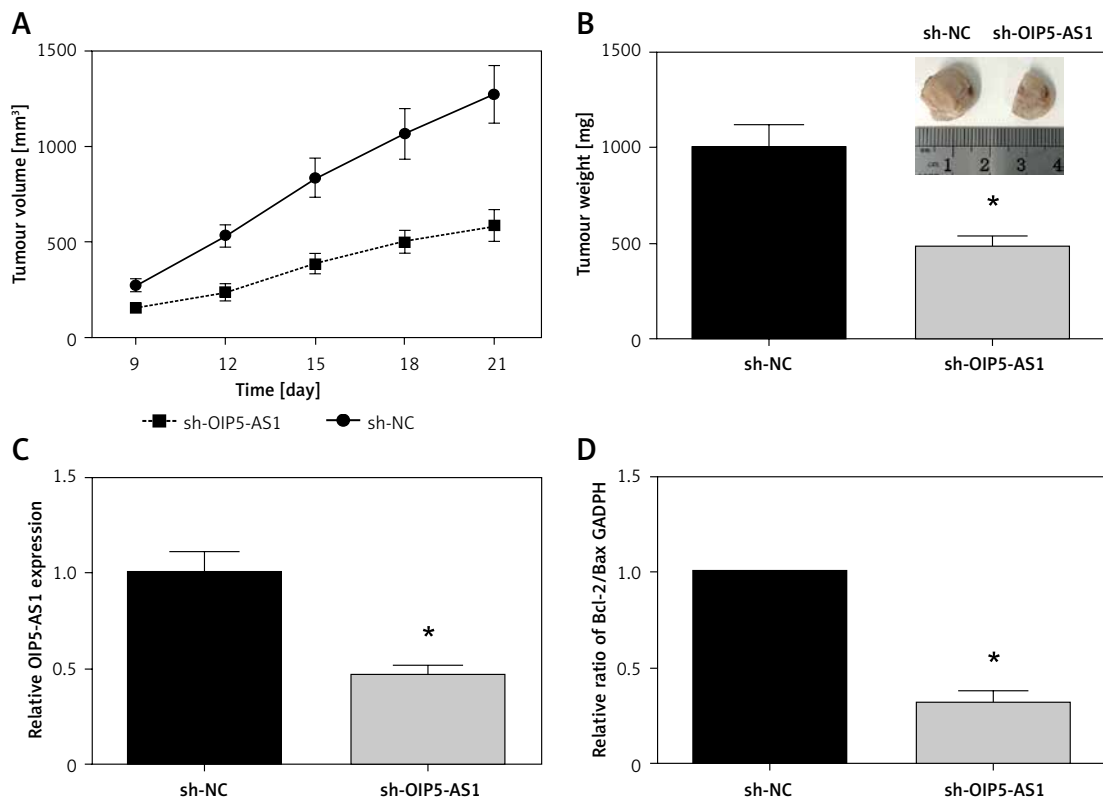


Figure 3. Knockdown of OIP5-AS1 inhibits GC tumour growth *in vivo*. **A** – Tumour volumes were measured every 3 days, and growth curves of tumours were plotted. **B** – The average weights of tumours were measured. **C** – The expression levels of OIP5-AS1 in the tumour tissues were examined by RT-qPCR analysis. **D** – The expression levels of Bax and Bcl-2 in the tumour tissues were detected by western blot analysis

* $p < 0.05$ vs. sh-NC group.

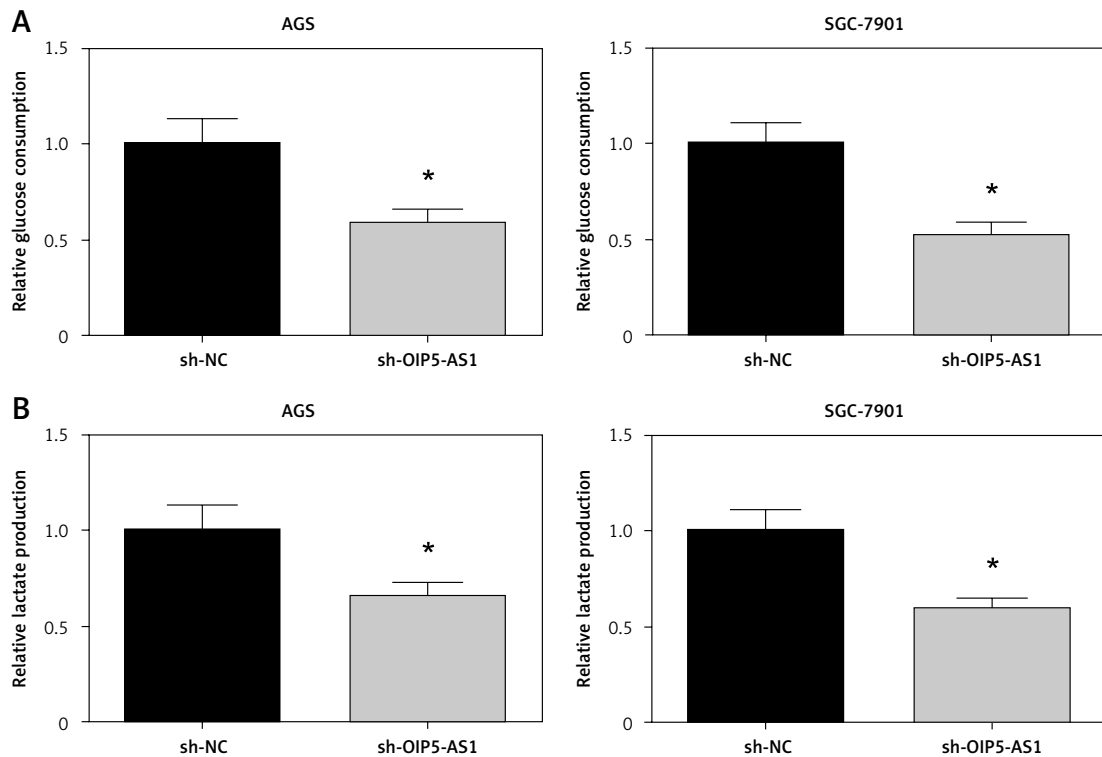
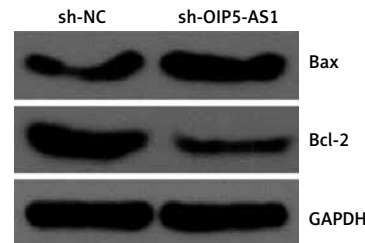


Figure 4. Knockdown of OIP5-AS1 suppresses aerobic glycolysis in GC cells. The glucose consumption (**A**) and lactate production (**B**) of AGS and SGC-7901 cells after transfection were detected by commercial kits

* $p < 0.05$ vs. sh-NC-transfected cells.

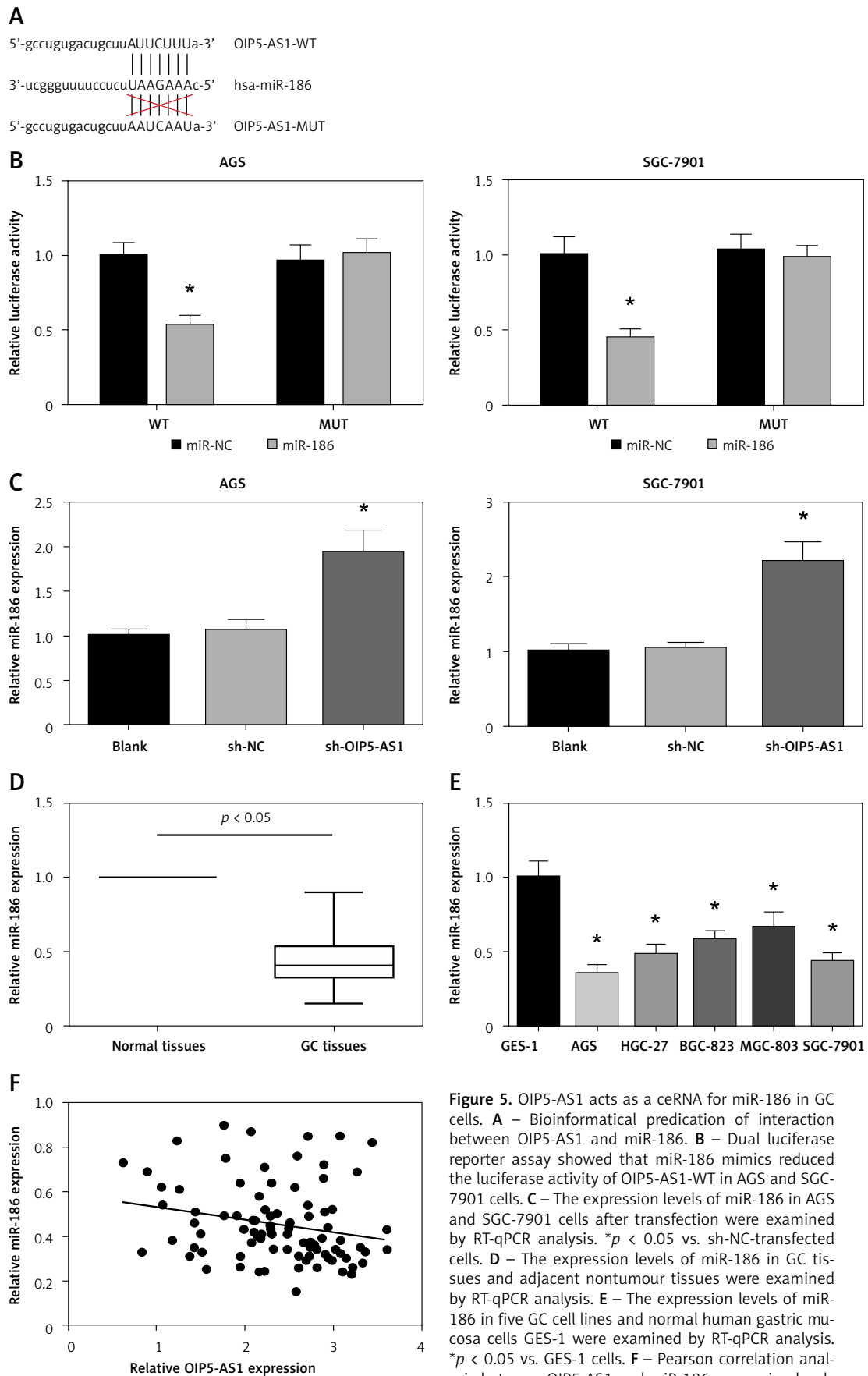


Figure 5. OIP5-AS1 acts as a ceRNA for miR-186 in GC cells. **A** – Bioinformatical predication of interaction between OIP5-AS1 and miR-186. **B** – Dual luciferase reporter assay showed that miR-186 mimics reduced the luciferase activity of OIP5-AS1-WT in AGS and SGC-7901 cells. **C** – The expression levels of miR-186 in AGS and SGC-7901 cells after transfection were examined by RT-qPCR analysis. * $p < 0.05$ vs. sh-NC-transfected cells. **D** – The expression levels of miR-186 in GC tissues and adjacent nontumour tissues were examined by RT-qPCR analysis. **E** – The expression levels of miR-186 in five GC cell lines and normal human gastric mucosa cells GES-1 were examined by RT-qPCR analysis. * $p < 0.05$ vs. GES-1 cells. **F** – Pearson correlation analysis between OIP5-AS1 and miR-186 expression levels in GC tissues

Discussion

Gastric cancer is a major threat to human health, and lncRNAs are important players in GC initiation and development [12]. For example, lncRNA CCAT1 was overexpressed in GC tissue samples compared to adjacent normal tissue samples [13], and lncRNA AFAP1-AS1 promotes the proliferation, migration, and invasion of GC cells [14]. In the present study, high expression of OIP5-AS1 in GC tissues and cell lines indicated that OIP5-AS1 might be an oncogene in GC. To further investigate the effects of OIP5-AS1 on GC cell phenotypes, OIP5-AS1 was knocked down in AGS and SGC-7901 cells, and we observed that OIP5-AS1 knockdown significantly inhibited GC cell proliferation and promoted GC cell apoptosis. In line with these findings *in vitro*, animal experimental study also validated the growth-inhibiting role of OIP5-AS1 knockdown.

The competing endogenous RNA (ceRNA) hypothesis is gaining attention for revealing the regulatory role of lncRNAs in GC [15, 16]. MicroRNAs (miRNAs), a class of small non-coding RNAs, also play a pivotal role in cancer biology [17], and

lncRNAs may function as a ceRNA to bind to miRNAs and negatively modulate their functions. In lung cancer, OIP5-AS1 functions as a ceRNA of miR-378a-3p [7]. This study identified miR-186 as a direct target of OIP5-AS1 by bioinformatic prediction based on sequence complementarity. The miR-186 was previously reported to be down-regulated in GC [18], and many lncRNAs, including PVT1 and ANRIL, play oncogenic roles through interaction with miR-186 [19, 20]. Here, we also observed that an inverse correlation existed between OIP5-AS1 and miR-186 expression in GC tissues. The interaction between lncRNAs and miRNAs provides new insights to elucidate the underlying mechanisms underlying GC progression.

Aerobic glycolysis, also termed the Warburg effect, is one of main metabolic characteristics of tumour cells, which is highlighted by the consumption of more glucose and the production of more lactate compared with normal cells, and therefore targeting aerobic glycolysis is a potential anticancer strategy [21, 22]. As indicated in our results, knockdown of OIP5-AS1 inhibited the glucose

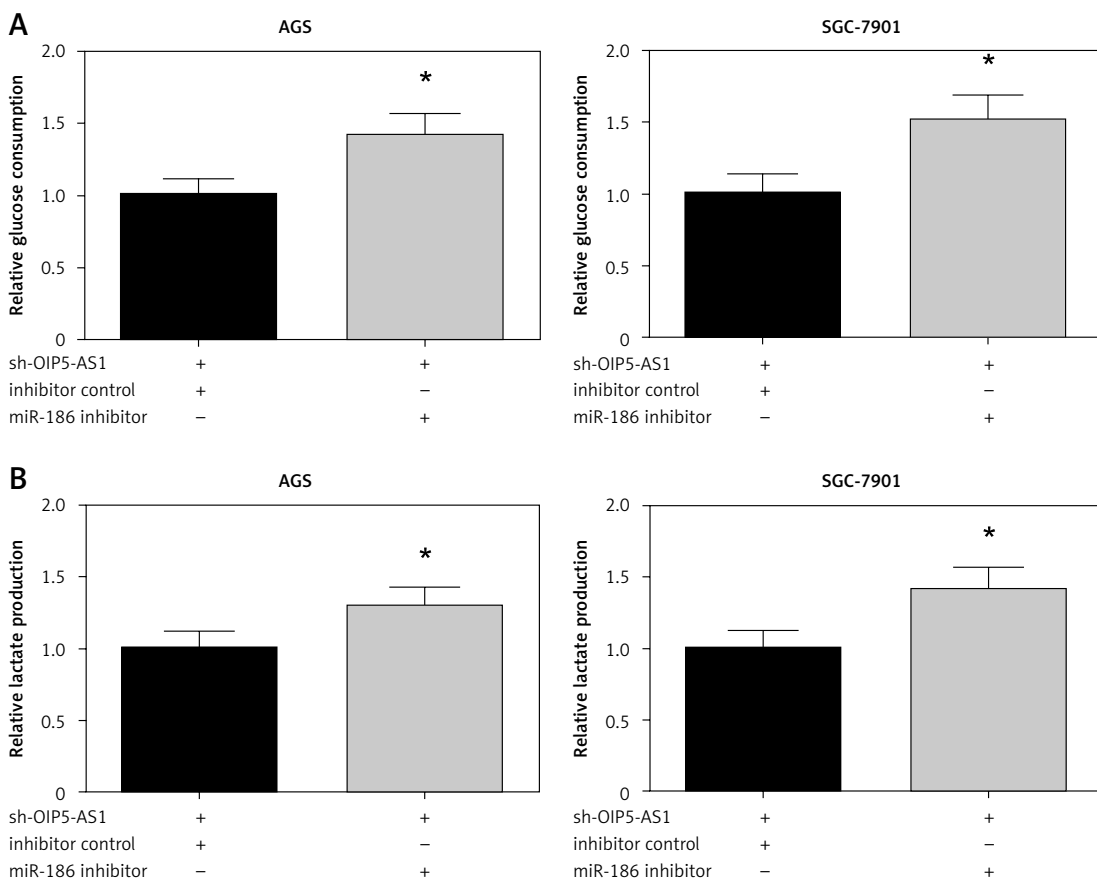


Figure 6. Inhibition of miR-186 attenuates the effect of OIP5-AS1 knockdown on aerobic glycolysis in GC cells. The glucose consumption (A) and lactate production (B) of AGS and SGC-7901 cells after transfection were detected by commercial kits

**p* < 0.05 vs. inhibitor control-transfected cells.

consumption and lactate production in GC cells. Liu *et al.* previously reported that overexpressed miR-186 inhibited aerobic glycolysis in GC cells [23], and consistently in this study we also found that miR-186 inhibition reversed the impaired aerobic glycolysis induced by OIP5-AS1 knockdown in GC cells. These findings clearly certified that OIP5-AS1 promotes aerobic glycolysis in GC cells partly through a manner found in ceRNA of miR-186.

In conclusion, the present study provided the first evidence that OIP5-AS1 was upregulated in GC tissues and cell lines. Moreover, knockdown of OIP5-AS1 inhibited GC cell proliferation *in vitro* and GC tumour growth *in vivo*. We further found that OIP5-AS1 might act as a ceRNA of miR-186, and the OIP5-AS1/miR-186 axis regulates aerobic glycolysis in GC cells. Our results indicate that OIP5-AS1 might serve as a potential therapeutic target for the treatment of GC.

Acknowledgments

Jiobao Huang and Shuangshuang Hou contributed equally to this work.

Conflict of interest

The authors declare no conflict of interest.

References

- Chen W, Zheng R, Baade PD, et al. Cancer statistics in China, 2015. *CA Cancer J Clin* 2016; 66: 115-32.
- Bertuccio P, Chatenoud L, Levi F, et al. Recent patterns in gastric cancer: a global overview. *Int J Cancer* 2009; 125: 666-73.
- Ponting CP, Oliver PL, Reik W. Evolution and functions of long noncoding RNAs. *Cell* 2009; 136: 629-41.
- Tang JY, Lee JC, Chang YT, et al. Long noncoding RNAs-related diseases, cancers, and drugs. *ScientificWorldJournal* 2013; 2013: 943539.
- Kim J, Noh JH, Lee SK, et al. LncRNA OIP5-AS1/cyranos suppresses GAK expression to control mitosis. *Oncotarget* 2017; 8: 49409-20.
- Deng J, Deng H, Liu C, Liang Y, Wang S. Long non-coding RNA OIP5-AS1 functions as an oncogene in lung adenocarcinoma through targeting miR-448/Bcl-2. *Biomed Pharmacother* 2018; 98: 102-10.
- Wang M, Sun X, Yang Y, Jiao W. Long non-coding RNA OIP5-AS1 promotes proliferation of lung cancer cells and leads to poor prognosis by targeting miR-378a-3p. *Thorac Cancer* 2018; 9: 939-49.
- Liu X, Zheng J, Xue Y, et al. PIWIL3/OIP5-AS1/miR-367-3p/CEBPA feedback loop regulates the biological behavior of glioma cells. *Theranostics* 2018; 8: 1084-105.
- Zhang Z, Liu F, Yang F, Liu Y. Knockdown of OIP5-AS1 expression inhibits proliferation, metastasis and EMT progress in hepatoblastoma cells through up-regulating miR-186a-5p and down-regulating ZEB1. *Biomed Pharmacother* 2018; 101: 14-23.
- Livak KJ, Schmittgen TD. Analysis of relative gene expression data using real-time quantitative PCR and the 2(-Delta Delta C(T)) method. *Methods* 2001; 25: 402-8.
- Vander Heiden MG, Cantley LC, Thompson CB. Understanding the Warburg effect: the metabolic requirements of cell proliferation. *Science* 2009; 324: 1029-33.
- Fang XY, Pan HF, Leng RX, Ye DQ. Long noncoding RNAs: novel insights into gastric cancer. *Cancer Lett* 2015; 356 (2 Pt B): 357-66.
- Li Y, Zhu G, Ma Y, Qu H. LncRNA CCAT1 contributes to the growth and invasion of gastric cancer via targeting miR-219-1. *J Cell Biochem* 2019; 120: 19457-68.
- Zhao H, Zhang K, Wang T, et al. Long non-coding RNA AFAP1-antisense RNA 1 promotes the proliferation, migration and invasion of gastric cancer cells and is associated with poor patient survival. *Oncol Lett* 2018; 15: 8620-6.
- Salmena L, Poliseno L, Tay Y, Kats L, Pandolfi PP. A ceRNA hypothesis: the Rosetta Stone of a hidden RNA language? *Cell* 2011; 146: 353-8.
- Hu Y, Tian H, Xu J, Fang JY. Roles of competing endogenous RNAs in gastric cancer. *Brief Func Genomics* 2016; 15: 266-73.
- Garzon R, Calin GA, Croce CM. MicroRNAs in cancer. *Ann Rev Med* 2009; 60: 167-79.
- Cao C, Sun D, Zhang L, Song L. miR-186 affects the proliferation, invasion and migration of human gastric cancer by inhibition of Twist1. *Oncotarget* 2016; 7: 79956-63.
- Huang T, Liu HW, Chen JQ, et al. The long noncoding RNA PVT1 functions as a competing endogenous RNA by sponging miR-186 in gastric cancer. *Biomed Pharmacother* 2017; 88: 302-8.
- Zhang JJ, Wang DD, Du CX, Wang Y. Long noncoding RNA ANRIL promotes cervical cancer development by acting as a sponge of miR-186. *Oncol Res* 2018; 26: 354-52.
- Koppenol WH, Bounds PL, Dang CV. Otto Warburg's contributions to current concepts of cancer metabolism. *Nat Rev Cancer* 2011; 11: 325-37.
- Yu L, Chen X, Wang L, Chen S. The sweet trap in tumors: aerobic glycolysis and potential targets for therapy. *Oncotarget* 2016; 7: 38908-26.
- Liu L, Wang Y, Bai R, Yang K, Tian Z. MiR-186 inhibited aerobic glycolysis in gastric cancer via HIF-1alpha regulation. *Oncogenesis* 2016; 5: e224.